Impedance based combination of visual and force control

G. Morel, Ezio Malis, S. Boudet

Impedance based combination of visual and force control

Guillaume Morel [†]
ENSPS/ LSIIT / GRAVIR
Bd Sébastien Brant
67400 Illkirch - France

Ezio Malis [†]
IRISA / INRIA
Campus de Beaulieu
F-35042 Rennes - France

Sylvie Boudet
EDF/ DER/ P29
6, Quai Watier
78401 Chatou - France

Abstract

In this paper, we propose a simple and efficient control algorithm that combines visual servo control and force feedback within the impedance control approach. The control scheme involves, at the low level, a position based impedance controller with an external force sensor feedback loop. The reference trajectory fed to this impedance controller is generated on line by a vision based control loop.

In spite of its simplicity, this approach provides satisfactory experimental behavior. Peg in hole insertion experiments involving large initial errors, are performed using a 7 axis robot manipulator without any computation of the peg trajectory.

1. Introduction

Most applications of advanced robotics, and particularly hazardous environment robotics, require to provide robot manipulators with the ability of working in environments with unknown location and geometry. Thus, external sensory information has to be integrated in the manipulator control.

Early in robot control development, force sensing capabilities have been considered as a crucial issue, as the robot often interacts with its environment. Many researches have been conducted to understand stability properties, bandwidth limitation, and to emphasize the role of dynamics in force control [1 - 4].

On another hand, vision based control has recently received a growing interest, as the computational power of commercially available computers became compatible with real time visual feedback [5 - 7].

For both vision and force control, initial drawbacks have been overpassed, and a number of techniques are now available. They shall be selected depending on the nature of the task, the robot and sensor design, and the low level controller hardware.

Our aim in this work was to exploit the vision based control and force control complementarity. While the robot is far from any physical constraints, eye-in-hand vision based control is useful for bringing parts to be mated into alignment. When the robot's tip gets close from the environment, unpredicted contacts can occur and involve large forces (Figure 1). It is expected that a force controller can then provide compliance to limit interaction forces and guide the manipulator to the final position. Although combining visual tracking capabilities with compliance has an obvious interest, only a little research has been conducted in this area.

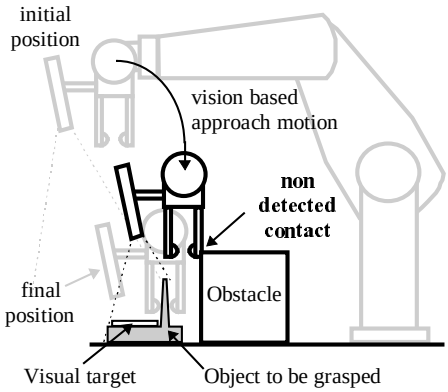

Figure 1 : Object grasping using vision based control

The first way of addressing multiple sensor feedback control is multi-sensory fusion. For example, it has been used in [8] to combine tactile and visual data. However, for the type of behavior we want to obtain, sensory fusion is conceptually inappropriate. The camera and the force sensor measure different physical phenomena (e.g. in Figure 1, the camera does not see the obstacle), while multi-sensory fusion is aimed in extracting a single information from disparate sensor data. In addition, interpreting real force / torque sensor data is extremely complex, particularly in the presence of friction, and when contact points locations are not known in advance.

Thus, it is preferable to directly combine *at the control level* the actions simultaneously commanded by a force controller and a vision based controller. This has been proposed in [9, 10] within the hybrid position / force control framework [3]. Force is controlled along constrained directions while the vision feedback controls the remaining degrees of freedom.

Hybrid position / force control does not fully exploit force and vision complementarity. The range of feasible tasks is reduced to those that can be described in terms of constraint surfaces. In [9, 10] applications are limited to a single contact point on a planar surface. Considering a realistic application with unknown constraint location and complex contact geometry, it is impossible to determine in advance a hybrid strategy, i.e. selection matrices and desired force/torque. In the general case, it is more suitable to use impedance control framework because it allows to *a priori* define the way the manipulator shall react with respect to unknown external

[†] G. Morel and E. Malis have performed this research at EDF - DER - Chatou.

force disturbances, while it can simultaneously be fed by a vision based reference trajectory along the six degrees of freedom.

This paper shows the implementation of this simple idea. Section 2 describes the different levels of the control structure. A controller analysis is developed in section 3 using the task-function concept [11]. Experiments are discussed in section 4.

2. Proposed control scheme

Impedance control approach is a way to provide the end effector with a programmable mechanical impedance :

$$F = \mathbf{M_d}\ddot{X} + \mathbf{B_d}\left(\dot{X}_r - \dot{X}\right) + \mathbf{K_d}\left(X_r - X\right) \qquad (1)$$

where F is the interaction wrench, X is the actual end-effector pose, X_r the reference trajectory. In our control structure, the reference trajectory is generated by the vision based controller that uses real time vision feedback.

The force feedback does not appear explicitly in Equation (1). Rather, it is used implicitly to achieve the specified target impedance, that is the desired mass matrix $\mathbf{M_d}$, damping matrix $\mathbf{B_d}$ and stiffness matrix $\mathbf{K_d}$.

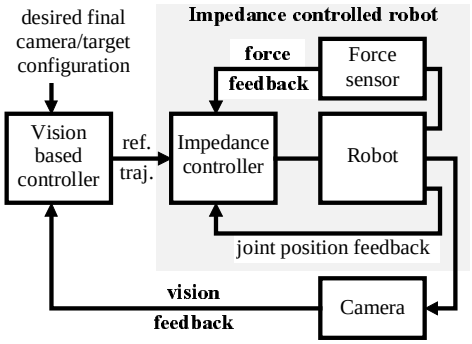

Figure 2 : Global structure of the controller.

The global structure of our controller is depicted in Figure 2. In the following sections, the design of the different control levels is detailed.

2.1 « Position based » impedance control

Impedance control can be achieved in numerous ways. They are usually classified in two main groups : force-based impedance control, in which the low level loop is a force loop, and position based control, which involves a low level position controller. As a general purpose, in terms of performances, force-based impedance control should be preferred, because it is able of providing a large range of target impedances, including soft behaviors [4].

However, stability robustness of force-based impedance control over the manipulator workspace is weak and a dynamic model is needed [12]. This leads to a complex control law, particularly for a redundant manipulator, as the one used in our application. Besides, force based impedance control is not relevant to most industrial applications, that use built-in joint position controllers in the robot's controller hardware. Furthermore, the tasks concerned by this work do not require high velocities, which means that a low bandwidth force response is acceptable.

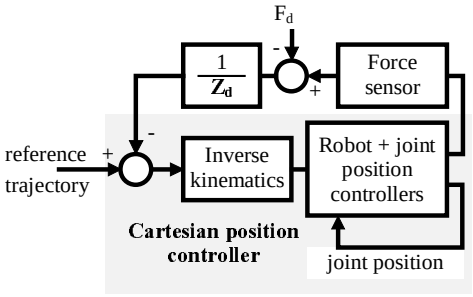

Figure 3 : Position-based impedance control

Thus, a position based impedance controller has been selected. Figure 3 depicts the impedance control scheme we have used. The joint redundancy of the robot is solved by minimizing joint velocities in the inverse kinematics procedure using a conventional pseudo inverse algorithm :

$$\dot{q}_c = \mathbf{J}^{+}\dot{X}_c \qquad (2)$$

In addition, a second order differential model is used to solve the inverse kinematics in singular joint configurations [13].

In the control scheme, a wrench input F_d is added in the force feedback loop, although initial statements (eq. 1) do not include such possibility. Note that this has no effect on closed loop behavior, since the wrench input can be viewed as a *reference trajectory modifier* [12].

Finally, for the experiments shown in this paper, the target impedance $\mathbf{Z_d}$ is limited to pure damping $\mathbf{B_d}$. Thus, the control law becomes :

$$\dot{X}_c = \dot{X}_r - \mathbf{B_d}^{-1}(F - F_d) \qquad (3)$$

which is also known as accommodation control [14].

2.2 Vision based external control

Vision based control can be achieved using mainly three different methods. In a *3D visual servoing* system, the error to be controlled corresponds to the camera's pose, that is its position and orientation [6]. The pose relative to the target is estimated from image features, which requires the precise knowledge of both the target geometry and the camera calibration parameters. Conversely, *2D visual servoing* exploits an error directly computed from the image features, relatively to their desired values [7]. Finally, in the *2D½ visual servoing* approach, the error to be controlled is computed in part in the cartesian space and in part directly in the image [15].

Any of the three methods could have been selected for our study as we are focused more on the force and vision combination issues than on the design of each separate level. The 2D servoing approach has been chosen because it is known to be very robust with respect to camera and robot calibration errors [5].

The implemented 2D visual controller, depicted in Figure 4, is given by :

$$\dot{X}_r = -\alpha \mathbf{C_v} \left(v - v_d\right) \tag{4}$$

where :

- v is the actual image feature and v_d its desired value. In the implemented controller, the image features are the image coordinates of the geometric centers of seven co-planar points constituting the target ;
- α is positive scalar that tunes the convergence rate;
- $\mathbf{C_v}$ is a combination matrix, that, ideally, reproduces the mapping between the image feature motion and the end effector motion.

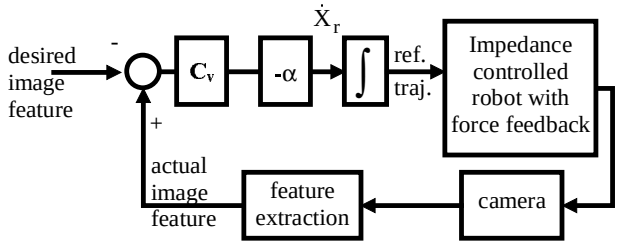

Figure 4 : 2D visual servoing

The optimal choice for $\mathbf{C_v}$ is given by :

$$\mathbf{C_v} = \mathbf{L_v^+} \tag{5}$$

Where $\mathbf{L_v}$ is the interaction matrix between the image feature and the robot motion. The expression of $\mathbf{L_v}$ can be found in [7] for different sorts of image feature. Of course, $\mathbf{L_v}$ is not exactly known in general. Furthermore, it cannot be computed on line if the camera-to-target distance information is not available. Rather, a constant matrix $\mathbf{C_v}$ computed for $v=v_d$ is used :

$$\mathbf{C_v} = \mathbf{L_v^+}(v = v_d) \tag{6}$$

This choice, approximating the sensor space to robot motion space mapping, is of particular importance. The task function design methodology used in the next section is a way of addressing this issue.

3. Stability analysis

3.1 Theoretical stability analysis

The above presented 2D visual controller is actually an application of the general task-function approach, which is a unified way of designing and analyzing external sensory based control [11].

In this approach, the task is described as a function of a (multi) sensor signal s and its desired value s_d :

$$e = \mathbf{C}\left(s - s_d\right) \tag{7}$$

C being a constant combination matrix. The main object of the task function approach is to regulate the task function e to zero.

A possible way is to achieve exponential convergence of the task function :

$$\dot{e} = -\lambda e \tag{8}$$

When applied to motion rate control, this is ideally achieved by the following control law :

$$\dot{X}_c = -\lambda \mathbf{L}^+ \mathbf{C}^+ e \tag{9}$$

where **L** is the interaction matrix, mapping the robot velocity into the sensor signal velocity ($\dot{s} = \mathbf{L}\dot{X}$). The control law (9) cannot be applied in general because **L** is not exactly known. Rather, a way of designing the sensor based controller is to choose a constant combination matrix **C** that can be viewed as an approximation $\hat{\mathbf{L}}^+$ of $\mathbf{L}^+$:

$$\mathbf{C} \triangleq \hat{\mathbf{L}}^+ \tag{10}$$

Thus, the actual control law, approximating (9), is :

$$\dot{X}_c = -\lambda e \tag{11}$$

One of the main interests of this approach is that a simple sufficient stability condition is given by :

$$\mathbf{CL} > 0 \tag{12}$$

which means that the approximation of the interaction matrix $\mathbf{C} = \hat{\mathbf{L}}^+$ has to conserve the global positivity of the system.

Our controller can be analyzed using this task-function approach. Indeed, combining (3) and (4), we get :

$$\dot{X}_c = -\alpha \mathbf{C_v} \left(v - v_d\right) - \mathbf{B_d}^{-1}(F - F_d) \tag{13}$$

This can be written as :

$$\dot{X}_c = -\lambda \mathbf{C}\left(s - s_d\right), \text{ with : } \begin{cases} s = \begin{bmatrix} v \\ F \end{bmatrix} \\ \mathbf{C} = \frac{1}{\lambda}\begin{bmatrix} \alpha \mathbf{C_v} & \mathbf{B_d}^{-1} \end{bmatrix} \end{cases} \tag{14}$$

The interaction matrix **L** describes the sensor signal variations with respect to the end-effector pose X.

$$\mathbf{L} = \begin{bmatrix} \begin{bmatrix} \frac{\partial v}{\partial X} \end{bmatrix} \\ \begin{bmatrix} \frac{\partial F}{\partial X} \end{bmatrix} \end{bmatrix} = \begin{bmatrix} \mathbf{L_v} \\ \\ \mathbf{L_F} \end{bmatrix} \tag{15}$$

Thus :

$$\mathbf{CL} = \frac{1}{\lambda}\begin{bmatrix} \alpha \mathbf{C_v} & \mathbf{B_d}^{-1} \end{bmatrix}\begin{bmatrix} \mathbf{L_v} \\ \mathbf{L_F} \end{bmatrix} = \frac{\alpha}{\lambda}\mathbf{C_v}\mathbf{L_v} + \frac{1}{\lambda}\mathbf{B_d}^{-1}\mathbf{L_F} \tag{16}$$

In (16), one can see that if $\mathbf{C_v}\mathbf{L_v}$ and $\mathbf{B_d}^{-1}\mathbf{L_F}$ are both definite positive, then the condition (12) is satisfied, as long as α and λ are chosen strictly positive. In other words, if the vision feedback and the force feedback are stable separately, then the overall scheme is stable.

We first consider the stability properties of the force feedback part of the controller. The interaction matrix $\mathbf{L_F}$ depends on both the geometry of the constraint and the contact mechanics. Thus, a general stability condition cannot be derived for any task.

From now on, we consider a contact point configuration. Thus, only linear forces f are considered, instead of the complete wrench F. If we assume elastic deformations and no friction, we get [16] :

$$\mathbf{L_f} = k\left[nn^T\right] \tag{17}$$

where n is the unitary vector normal to the contact surface and k is the scalar stiffness. Since the desired damping is a constant spherical matrix, $\mathbf{B_d} = b_d\mathbf{I_3}$, we finally get :

$$\mathbf{B_d}^{-1}\mathbf{L_f} = \frac{k}{b_d}\left[nn^T\right] \tag{18}$$

which is positive for any positive value of b_d.

We now examine the stability properties for the vision based control. The choice of equation (6) implies that the condition $\mathbf{C_v L_v}>0$ is only satisfied in a neighborhood of the desired position. This condition is only sufficient and experimental results have shown that the convergence can be obtained for a large range of camera displacements [7].

Finally, both the force controller and the vision controller are stable separately. Thus, from (16), the overall controller is stable.

3.2 Practical stability issues

In the previous section, the stability has been analyzed from a theoretical point of view. Some practically important aspects have not been addressed.

Firstly, the inner cartesian position loop dynamics has been neglected, by formulating the problem as motion rate control. In practice though, the close loop position bandwidth does not exceed a few Hertz depending on the joint configuration. Thus, the stability proof applies only for sufficiently small force and vision feedback gains, which practically limits the overall bandwidth.

Secondly, the theoretical analysis has neglected contact friction. In practice, though, friction can significantly affects the system behavior.

Consider, for example, that reaching the target requires to move the end effector parrallelly to the contact surface. Without friction, the vision system guides the end-effector to the final position while slipping over the surface. However, in the presence of friction, the controller would fail. Close from the final position, the tangential velocity, commanded by the vision based controller decreases. At some point, it will become smaller than the opposite tangential velocity generated through the force feedback, due to friction component.

With a pure damping impedance, the following condition has to be respected to prevent the system from blocking :

$$\left|{}^t\dot{X}_{vision}\right| > \left|{}^t\dot{X}_{force}\right| = \mathbf{B_d}\left|{}^tF\right| \tag{19}$$

It is clear that with a proportional visual control law (Eq. 4), friction generates static positioning error. A Proportional Integral controller could be used but combining the integral correction with vision feedback and friction non linearities could lead to instability. Furthermore, limit cycles would appear. Rather, a dead zone in the force feedback loop can be used. If the force (in any direction) is smaller than a predetermined limit value, then the velocity commanded by the force loop is zero. This strategy has appeared to be efficient in practice.

4. Experiments

4.1 Experimental setup

Figure 5 depicts the experimental setup used in this work. The robot is a 7 axis redundant electric Mitsubishi PA-10 manipulator. A Panasonic camera and an ATI 6 axis force / torque sensor are mounted at the end-effector.

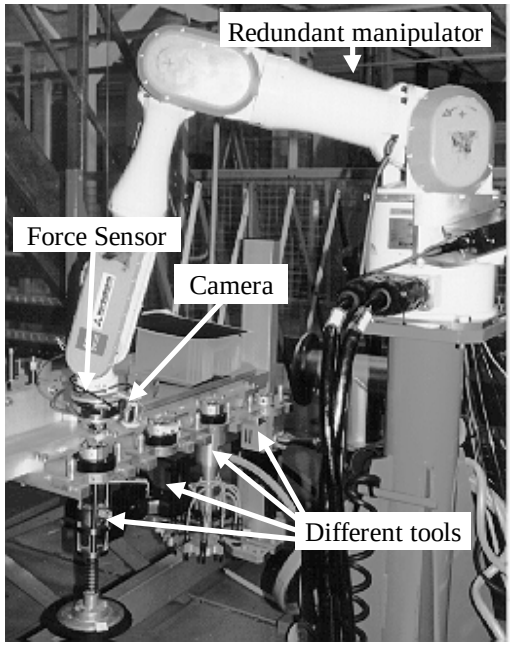

Figure 5 : General view of the experimental setup

Low level joint position control is achieved in the Mitsubishi controller, which communicates with a VME bus controller through an Arcnet communication link. Two CPU boards supporting VxWorks realize the position based impedance control. An additive specific EDIXIA vision dedicated board generates the reference velocity.

The illustrative task is a part of a real nuclear power plant valve maintenance operation. In order to be able to use the different tools involved in this task (see Figure 5),

a female interface is mounted on each tool, that matches the end-effector mounted electro-pneumatic male tool changer. The clearance is less than a tenth millimeter, and the tool location is unknown. A detailed view of the tool changer mounted on the robot's end-effector is given in Figure 6.

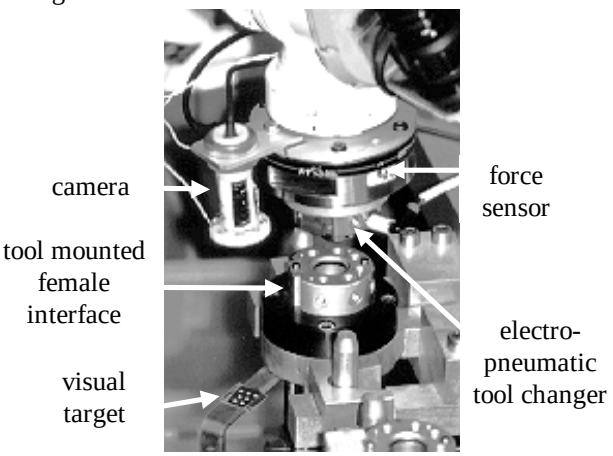

Figure 6 : Detailed view of the task

4.2 Experimental methodology

Associated with our controller, a simple programming methodology has been developed. It uses two steps :

1. The task in run *manually*, that is the impedance control is running, but the reference trajectory is provided by a teleoperation device instead of the vision servo controller.
2. Once the desired final position is reached, and the force feedback loop is stabilized to zero, the image feature is computed and stored in the memory.

In order to be able to reach this position through combined visual and force control, one simply set the desired image feature to the memorized value, while the desired force is set to zero. Thus, programming a task as complex as tool changer insertion is extremely simple.

4.3 Results

To illustrate the experimental behavior of our approach, we compare two tool changer insertion attempts. The first one is done with pure visual servoing, while the second one uses combined force and vision control.

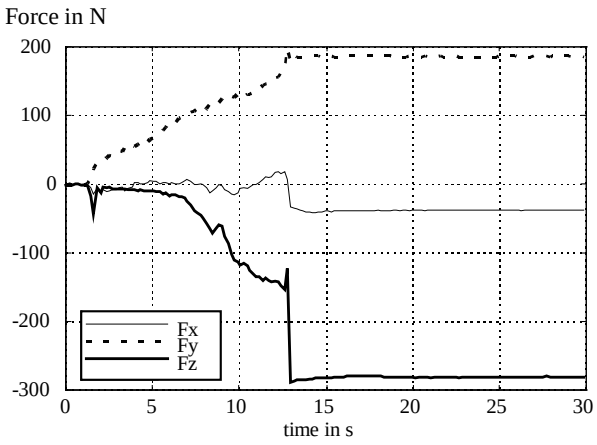

Figure 7 : Forces with pure visual servo control
(Z = insertion axis, X and Y ∈ perpendicular plane)

In both experiments, the initial position is reached with vision based control, in order to place the tool changer exactly in front of the female interface. The insertion motion is then a pure translation along the insertion axis, which corresponds to the easiest configuration. In a perfect world, the contact force should stay null. However, the vision based control does not generate a straight line trajectory. As a matter of fact, the trajectory is generated in order to minimize the image feature error, not the end effector position error. All the geometric modeling errors in both the robot and the sensory system contributes to amplify the deviation from the ideal straight line trajectory. Thus, contact forces appear.

Figure 7 shows an example result for pure vision based insertion. Due to the integral effect of the visual control, combined to the rigidity of the parts to be mated, the force increases rapidly.

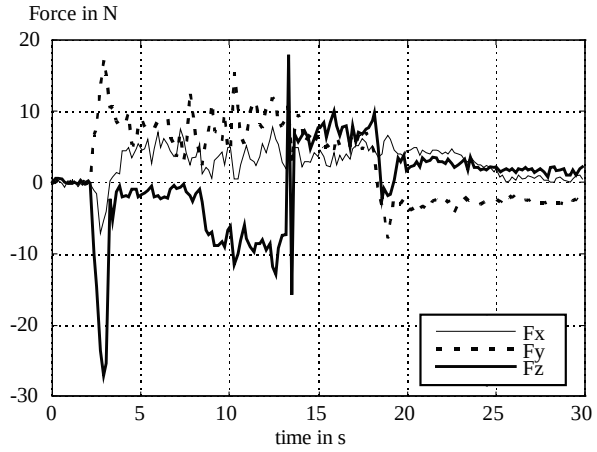

Figure 8 : Forces evolution during peg-in-hole insertion with combined visual and force control

At t ≅ 13 seconds, as the end-effector almost reaches the final position, the electro-pneumatic tool changer is actuated. The sudden change in contact forces is mainly due to the grasped tool weight. Once the tool is grasped,

the vision system detects final convergence and the robot remains immobile. One can see that the forces involved during the task are large. Actually, they exceed the maximum value recommended by the robot constructor.

Conversely, when the same experiment is performed with combined active compliance, the force remains small. In Figure 8, the force is reduced by a factor 9 (note the change in the coordinates scale).

5. Conclusion

There are obvious advantages in combining vision and force feedbacks in the control of a robot manipulator. Though, we have found only very few proposals in the literature. Previous work was based on hybrid position / force control, which does not entirely exploit the interest of sensors duality. Our paper has proposed to combine vision and force control within the impedance control approach.

The implemented control scheme involves a pure damping position-based impedance control and an external image-based visual controller. It is simple and practical, because the impedance controller and the vision based controller can be designed separately, as shown by the stability analysis.

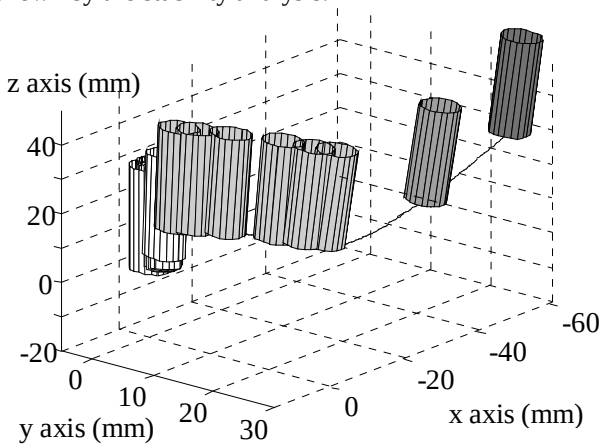

Figure 9 : Peg trajectory, reconstructed from experimental data.

Experimental results given in section 4 show that the force feedback can compensate for the forces undesirably generated by the 2D visual feedback. Additional extensive experiments pointed out that the force and vision combination is not limited to this.

In Figure 9, the insertion experiment was realized with a very large initial positioning error, in both position and orientation. It is clear that, since the hole location is completely unknown, force control alone is absolutely not capable of performing this task. On the other hand, if we wanted to realize the assembly with a pure visual feedback, we would have to use 3D vision and to compute the insertion trajectory in advance, with respect to the geometry of the parts to be mated.

Conversely, Figure 9 shows that our control scheme is capable of performing low clearance peg-in-hole tasks, with significant initial errors in all the 6 degrees of freedom, and without any knowledge of the hole location, nor on the constraint geometry. No trajectory computation, nor complex insertion strategy is required, as the only input is the final desired image feature vector and the desired force.

References

[1] S.D. Eppinger and W.P Seering., Three dynamic problems in robot force control, *Proc. of IEEE Int. Conf. on Robotics and Automation*, pp392-397, 1989.

[2] O. Khatib, A unified approach for motion and force control : the operational space formulation, *IEEE Trans. on Robotics and Automation*, 3 (3) : 43-53, 1987.

[3] M.H. Raibert and J.J. Craig, Hybrid position/force control of manipulators, *ASME Journal of Dynamic Systems, Measurement and Control*, vol. 102, pp 126-133, 1981.

[4] D. Lawrence, Impedance control stability properties in common implementations, *Proc. of the IEEE Int. Conf. on Robotics and Automation*, pp 1185-1192, 1988.

[5] S. Hutchinson, G.D. Hager and P.I. Corke, A tutorial on visual servo control, *IEEE Trans. on Robotics and Automation*, 12 (5) : 651-670, 1996.

[6] W.J. Wilson, C.C.W. Hulls and G.S. Bell, Relative end-effector control using cartesian position based visual servoing, *IEEE Trans. on Robotics and Automation*, 12 (5) : 684-696, 1996.

[7] B. Espiau, F. Chaumette and P. Rives, A new approach to visual servoing in robotics. *IEEE Trans. on Robotics and Automation*, 8 (3) : 313-326, 1992.

[8] R. Bajcsy, Integrating vision and touch for robotic applications, *Trends and Applications of AI in Business*, ed. W. Reitman, Ablex Publ. Co., 1984.

[9] B.J. Nelson and P.K. Khosla, Force and vision resolvability for assimilating disparate sensory feedback, *IEEE Trans. on Robotics and Automation*, 12 (5) : 714-731, 1996.

[10] K. Hosoda, K. Igarashi and M. Asada, Adaptive hybrid visual servoing / force control in unknown environment, *Proc. of IEEE/RSJ International Conference on Intelligent Robots and Systems*, pp. 1097-1103, 1996.

[11] C. Samson, M. Leborgne and B. Espiau, *Robot control : the task function approach*, Clarendon Press, Oxford Science Publications, 1991.

[12] G. Morel and P. Bidaud, A reactive external force loop approach to control manipulators in the

presence of environmental disturbances, *Proc. of the IEEE Int. Conf. on Robotics and Automation*, pp 1229-1234, 1996.

[13]E. Malis, L. Morin and S. Boudet, Control of redundant robots at singularities in degenerate directions, *Proc. of the 12th CISM-IFToMM Symp. on Theory and Practice of Robots and Manipulators,* pp 319-326, 1996.

[14]D.E. Whitney, Force feedback control of manipulator fine motions, *Journal of Dynamic Systems, Measurement and Control,* pp 91-97, 1977.

[15]E. Malis, F. Chaumette and S. Boudet, Positioning a coarse-calibrated camera with respect to an unknown planar object by 2D ½ visual servoing, *Preprints of the 5th Symposium on Robot Control, SyRoCo'97* , pp 517-523, 1997

[16]B. Espiau, JP Merlet and C. Samson, Force-feedback control and non-contact sensing: a unified approach , Proc. *of the 8th CISM-IFTOMM Symp. on Theory and Practice of Robots and Manipulators, Ro'Man'Sy'90*, 1990.